Available online at www.sciencedirect.com
SCIENCE DIRECT®
International Journal of Heat and Mass Transfer 48 (2005) 3957–3970
International Journal of HEAT and MASS TRANSFER
www.elsevier.com/locate/ijhmt

Numerical analysis of heat transfer in pulsating turbulent flow in a pipe

Xuefeng Wang [a], Nengli Zhang [b,*]

[a] Department of Mechanical Engineering, University of Nebraska, Lincoln, NE 68588, USA
[b] NASA Glenn Research Center at Lewis Field, Microgravity Science Division, 21000 Brookpark Road, Cleveland, OH 44135, USA

Received 5 October 2004; received in revised form 15 April 2005
Available online 29 June 2005

Abstract

Convection heat transfer in pulsating turbulent flow with large velocity oscillating amplitudes in a pipe at constant wall temperature is numerically studied. A low-Reynolds-number (LRN) k–ε turbulent model is used in the turbulence modeling. The model analysis indicates that Womersley number is a very important parameter in the study of pulsating flow and heat transfer. Flow and heat transfer in a wide range of process parameters are investigated to reveal the velocity and temperature characteristics of the flow. The numerical calculation results show that in a pulsating turbulent flow there is an optimum Womersley number at which heat transfer is maximally enhanced. Both larger amplitude of velocity oscillation and flow reversal in the pulsating turbulent flow also greatly promote the heat transfer enhancement.

Keywords: Convection heat transfer; Pulsating flow; Turbulent modeling; Large velocity amplitude; Womersley number; Numerical calculation

1. Introduction

Periodic fluctuations of fluid flow create different characteristics of flow and heat transfer. Generally, the flow fluctuations are divided into two categories: pulsating flow (or pulsatile flow) in which the periodically time-averaged velocity is non-zero and oscillating flow (or oscillatory flow) in which the periodically time-averaged velocity is zero. Pulsating fluid flow and heat transfer occur in many industrial products, such as pulse combustor for both civil and military uses, reciprocating engine, ramjet, cooling system for nuclear reactor, etc. In addition, the circulation of blood in human body is also a typical process of pulsating flow and heat transfer. Heat transfer in pulsating laminar flow has been studied by many investigators. However, heat transfer in pulsating turbulent flow is more interesting and important in practical applications. Unfortunately, it is still lacking in study.

Experimental studies on pulsating turbulent flow were conducted actively [1–10]. All of the measurements were made for fully developed flows with small oscillating velocity amplitudes. Heat transfer in pulsating turbulent flow was also experimentally studied and a variety of confusable results were reported: the

* Corresponding author. Tel.: +1 216 433 8750; fax: +1 216 433 8050.
E-mail address: nengli.zhang@grc.nasa.gov (N. Zhang).

0017-9310/$ - see front matter © 2005 Elsevier Ltd. All rights reserved.
doi:10.1016/j.ijheatmasstransfer.2005.04.011

Nomenclature

A_T	oscillating amplitude of inlet temperature
A_u	oscillating amplitude of inlet velocity
c_p	specific heat at constant pressure (J/kgK)
C	constant in inlet turbulent energy dissipation rate
C_1, C_2, C_μ	empirical constants of k–ε model
D	diameter of pipe (m)
f	function in the correlation formula given by Petukhov and Popov
f_1, f_2, f_μ	turbulent model functions of k–ε model
G	production of turbulent kinetic energy (W/m^3)
h	instantaneous local heat transfer coefficient (W/m^2 K)
h_t	instantaneous heat transfer coefficient which is the average of heat transfer coefficient over the whole length of pipe at a given moment, $\frac{1}{L}\int_0^L h\,\mathrm{d}x$ (W/m^2 K)
h_x	local heat transfer coefficient which is the average of heat transfer coefficient over a cycle, $\frac{1}{2\pi}\int_0^{2\pi} hd(\omega t)$ (W/m^2 K)
k	turbulent kinetic energy (m^2/s^2)
K	thermal conductivity of fluid (W/m K)
L	length of pipe (m)
Nu	overall Nusselt number
Nu_t	instantaneous Nusselt number
Nu_{corl}	Nusselt number of fully developed turbulent pipe flow determined by correlation
Nu_x	local Nusselt number
$Nu_{x,t}$	instantaneous local Nusselt number, hD/K
p	pressure (N/m^2)
Pr	Prandtl number, ν/α
r	radial coordinate (m)
R	radius of pipe (m)
Re	Reynolds number, UD/ν
R_t	turbulent Reynolds number, $k^2/\nu\varepsilon$
s	period (s)
t	time (s)
T	temperature (°C)
T_{av}	average temperature along cross-sectional area of the pipe (°C)
u	velocity in x direction (m/s)
u_τ	wall-friction velocity, $\sqrt{\tau_w/\rho}$ (m/s)
U	periodically time-average of mean velocity at $x = 0$ (m/s)
v	velocity in r direction (m/s)
Wo	Womersley number, $R\sqrt{\omega/\nu}$
x	axial coordinate (m)
y	distance from wall (m)
y^+	dimensionless distance from wall, yu_τ/ν

Greek symbols

α	thermal diffusivity of fluid, $K/\rho c_p$ (m^2/s)
γ	relative error
ε	turbulent energy dissipation rate (W/kg)
Θ	periodically time-average of mean temperature at $x = 0$ (°C)
μ	dynamic viscosity (kg/ms)
μ_t	eddy (or turbulent) viscosity (kg/ms)
ν	kinematic viscosity (m^2/s)
ρ	density (kg/m^3)
σ_k	turbulent Prandtl number for k
σ_T	turbulent Prandtl number for T
σ_ε	turbulent Prandtl number for ε
τ_w	wall shear stress (N/m^2)
ω	angular frequency (1/s)

Subscripts

0	inlet
c	centerline
s	steady state flow
t	instantaneous
w	wall
x	position x

Superscripts

–	time-average
*	dimensionless variable

frequency had no direct effect on the Nusselt number [11], no heat transfer enhancement was found [12,13], a slight heat transfer reduction was found [14], the change in Nusselt number was negative below a certain frequency and positive above it [15], heat transfer enhancement could occur only when the oscillating frequency was higher than a certain value [16,17], the heat transfer coefficient increased with the pressure oscillation amplitude [18], high frequencies and large oscillation amplitudes promoted heat transfer enhancement, especially at low Reynolds numbers [19], Nusselt number was found to increase with both pulsation amplitude and frequency in a square-sectional duct [20] and so on. Among those experiments, most studies were performed under the condition of small oscillating velocity amplitudes except the works reported in Refs. [20,21]. Recently, Gbadebo et al. [22] experimentally studied heat transfer in the thermal entrance region of pulsating turbulent pipe flows under uniform heat flux conditions. They found that the average Nusselt number increased first and then decreased with the increase in frequency, implying the heat transfer was enhanced at medium

frequencies and reduced at both higher and lower frequencies within their experimental ranges. Unfortunately, in many articles, some important parameters were not considered. For example, oscillating amplitudes were not given in Ref. [15,19,22,23]. Consequently, the empirical correlations for Nusselt numbers obtained by these investigators do not contain any parameter involving the oscillating amplitude [22,23].

The analysis methods for the processes of pulsating turbulent flow and heat transfer can be classified into two categories: quasi-steady state theory [16,24–26] and turbulent modeling [27–31]. In view of the quasi-steady state theory is only suitable to pulsating flow with very low oscillating frequencies, several numerical studies with eddy viscosity models have been conducted for pulsating flow with higher frequencies. Andre et al. [27] numerically solved momentum and energy equations for hydrodynamically fully developed and thermally developing pulsating turbulent duct flow using mixing length (zero-equation model). For pulsating flow with large oscillation amplitude, the mixing length hypothesis becomes unpractical because it is difficult to find a formula to calculate the mixing length for flow reversal. Valueva et al. [28,29] numerically studied heat transfer in pulsating turbulent flow with velocity oscillation amplitudes up to 0.9 in a round tube treating the momentum and energy equations as parabolic ones. In fact, their model just is a kind of zero-equation model. Thyageswaran [30] used k–ε two-equation model and wall function method to study heat transfer in pulse combustor tail pipe. Due to the wall function k–ε model failed to predict the time-resolved variations of velocity and heat transfer rate, a boundary layer wall model was applied. Scotti and Piomelli [31] investigated four low-Reynolds-number turbulent models in pulsating flows, and found that all of them perform similarly with acceptable accuracies as long as the streamwise velocity is concerned.

The available literature shows that pulsating turbulent pipe flow and heat transfer are affected mainly by the following parameters: oscillating frequency, oscillating amplitude, Reynolds number, and Prandtl number. Pulsation patterns, such as the square wave and the sinusoidal wave that is most widely used, also affect the heat transfer enhancement. In addition, the location of pulsation source, upstream or downstream of the pulsating flow, has a direct effect on the heat transfer improvement [19]. In view of the effect of apparatus size on the experimental results, the Womersley number, instead of oscillating frequency, should be considered in the analysis of pulsating flow and heat transfer. In the previous experimental studies, almost all flow measurements in pulsating turbulent flows were performed for the developed flow with small velocity oscillating amplitudes. It is reasonable to expect that larger velocity oscillation amplitudes would produce stronger heat transfer enhancement [24,25].

When comparing the various studies on the heat transfer enhancement in pulsating flows, several confusable parameters should be carefully treated: (a) some authors discussed Nusselt number at fully developed region and others focused on Nusselt number averaged along axial length; (b) in some papers, the parameter "oscillating amplitude" is not a real velocity oscillating amplitude. Instead, it may be a combination of frequency and oscillation displacement or the ratio of the maximum displacement at the centerline to that in steady flow; and (c) different definitions of Nusselt number were used.

Due to the complexity of the turbulent fluid flow, studies on heat transfer in pulsating turbulent flow are far from matured. The available research results of the heat transfer enhancement show conflicts with each other. Both the mechanism of the heat transfer enhancement and the relationship between the heat transfer enhancement and the main processing parameters are not yet clear. In the theoretical studies, the quasi-steady state theory can only be applied to the cases of pulsating flows with very low oscillation frequencies.

In this paper, a numerical study on heat transfer in pulsating turbulent pipe flow over a wide range of Womersley number with large oscillating velocity amplitudes ($A_u > 1$) is reported. A two-dimensional model with elliptic differential equations in the cylindrical coordinate system is established and numerically solved. Unsteady Reynolds-averaged Navier–Stokes equations and a low-Reynolds-number k–ε turbulent model are applied.

2. Model analysis

A circular pipe with radius R and length L is chosen and the pulsating source of the flow is placed at the inlet of the pipe. Due to the axisymmetry, the problem can be considered to be two-dimensional and only a half cylindrical region is concerned, as shown in Fig. 1, where x is the axial coordinate and r is the radial coordinate. The working fluid is air and all thermophysical properties are assumed to be constant. The ratio of length to radius of the pipe, L/R, is set to be 200, so that the pipe is long enough to consider the flow both hydrodynamically and thermally fully developed in the pipe.

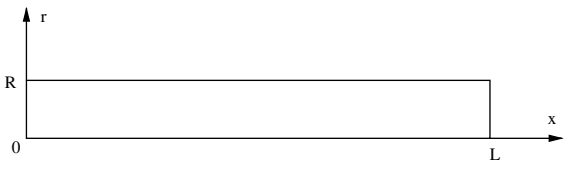

Fig. 1. Problem schematic.

2.1. Governing equations

Heat transfer in a pulsating pipe flow is governed by the Navier–Stokes and energy equations. For turbulent flows, the time-average values of velocity, pressure and temperature are the most important parameters for the analysis in engineering. It should be noted that the term "time-average" instead of "ensemble-average" is used here because from mathematics point of view, time-average is for continuous function and ensemble-average is for discrete function. Although the word "ensemble-average" is frequently used in fluid mechanics, it is not accurate to define the relevant parameters in the present study. Based on the physical model, with Boussinesq viscosity model, transient two-dimensional governing equations in the cylindrical coordinates are:

Continuity equation

$$\frac{\partial \bar{u}}{\partial x}+\frac{1}{r}\frac{\partial}{\partial r}(r\bar{v})=0, \tag{1}$$

where $\bar{u}$ is the time-average velocity in x-direction, $\bar{v}$ is the time-average velocity in r-direction.

Momentum equation in x-direction

$$\begin{aligned}&\frac{\partial(\rho\bar{u})}{\partial t}+\frac{\partial(\rho\bar{u}\bar{u})}{\partial x}+\frac{1}{r}\frac{\partial}{\partial r}(r\rho\bar{v}\bar{u})\\&\quad=-\frac{\partial\bar{p}}{\partial x}+\frac{\partial}{\partial x}\left((\mu+\mu_t)\frac{\partial\bar{u}}{\partial x}\right)+\frac{1}{r}\frac{\partial}{\partial r}\left(r(\mu+\mu_t)\frac{\partial\bar{u}}{\partial r}\right)\\&\qquad+\frac{\partial}{\partial x}\left((\mu+\mu_t)\frac{\partial\bar{u}}{\partial x}\right)+\frac{1}{r}\frac{\partial}{\partial r}\left(r(\mu+\mu_t)\frac{\partial\bar{v}}{\partial x}\right),\end{aligned} \tag{2}$$

where ρ is the density, $\bar{p}$ is the time-average pressure, μ is the dynamic viscosity, μ_t is the eddy viscosity.

Momentum equation in r-direction

$$\begin{aligned}&\frac{\partial(\rho\bar{v})}{\partial t}+\frac{\partial(\rho\bar{u}\bar{v})}{\partial x}+\frac{1}{r}\frac{\partial}{\partial r}(r\rho\bar{v}\bar{v})\\&\quad=-\frac{\partial\bar{p}}{\partial r}+\frac{\partial}{\partial x}\left((\mu+\mu_t)\frac{\partial\bar{v}}{\partial x}\right)+\frac{1}{r}\frac{\partial}{\partial r}\left(r(\mu+\mu_t)\frac{\partial\bar{v}}{\partial r}\right)\\&\qquad+\frac{\partial}{\partial x}\left((\mu+\mu_t)\frac{\partial\bar{u}}{\partial r}\right)+\frac{1}{r}\frac{\partial}{\partial r}\left(r(\mu+\mu_t)\frac{\partial\bar{v}}{\partial r}\right)\\&\qquad-\frac{2(\mu+\mu_t)\bar{v}}{r^2},\end{aligned} \tag{3}$$

and energy equation

$$\begin{aligned}&\frac{\partial(\rho\overline{T})}{\partial t}+\frac{\partial(\rho\bar{u}\overline{T})}{\partial x}+\frac{1}{r}\frac{\partial}{\partial r}(r\rho\bar{v}\overline{T})\\&\quad=\frac{\partial}{\partial x}\left(\left(\frac{\mu}{Pr}+\frac{\mu_t}{\sigma_T}\right)\frac{\partial\overline{T}}{\partial x}\right)+\frac{1}{r}\frac{\partial}{\partial r}\left(r\left(\frac{\mu}{Pr}+\frac{\mu_t}{\sigma_T}\right)\frac{\partial\overline{T}}{\partial r}\right),\end{aligned} \tag{4}$$

where $\overline{T}$ is the time-average temperature, Pr is the Prandtl number, σ_T is the turbulent Prandtl number for temperature T, defined as the ratio of the eddy viscosity to the turbulent diffusion coefficient for temperature. Body forces and viscous dissipations are neglected here.

2.2. Turbulent model

Among the available turbulent models, those based on the eddy viscosity are widely applied. The turbulent kinetic energy-turbulent energy dissipation rate (k–ε) two-equation model is a good representative. As is well known, the so-called standard k–ε model is valid only at high turbulent-Reynolds-number, i.e., the turbulent Reynolds number $R_t = k^2/\nu\varepsilon \gg 1$, where k is the turbulent kinetic energy, ν is the kinematic viscosity, and ε is the turbulent energy dissipation rate. Only with the help of wall function method can the standard k–ε model be applied to the near wall region. Such a method dominated computational analysis of turbulent flow till the 1970s. Jones and Launder [32,33] improved the k–ε model so that it can be valid in the low-Reynolds-number (low R_t) region, which occurs in the vicinity of the wall. It is called low-Reynolds-number (LRN) k–ε model. As pointed out by Patel et al. [34] in their review on LRN turbulent models, one of the shortcomings of this model is a lot of grid points have to be deployed in the near wall region, which calls for a high quality computer. Unless and until nowadays this model can be practically used with the help of supercomputers. In recent years, several other LRN k–ε models have been proposed. In the present study, the LRN k–ε model developed by Torii and Yang [35] is used. This model is summarized as follows.

Eddy viscosity formula

$$\mu_t = C_\mu f_\mu \rho\frac{k^2}{\varepsilon}, \tag{5}$$

where C_μ is an empirical constant, f_μ is the turbulent model function.

k-equation

$$\begin{aligned}&\frac{\partial(\rho k)}{\partial t}+\frac{\partial(\rho\bar{u}k)}{\partial x}+\frac{1}{r}\frac{\partial}{\partial r}(r\rho\bar{v}k)\\&\quad=\frac{\partial}{\partial x}\left(\left(\mu+\frac{\mu_t}{\sigma_k}\right)\frac{\partial k}{\partial x}\right)+\frac{1}{r}\frac{\partial}{\partial r}\left(r\left(\mu+\frac{\mu_t}{\sigma_k}\right)\frac{\partial k}{\partial r}\right)\\&\qquad+G-\rho\varepsilon,\end{aligned} \tag{6}$$

where σ_k is the turbulent Prandtl number for k, defined as the ratio of the eddy viscosity to the turbulent diffusion coefficient for k, G is the production of turbulent kinetic energy defined as

$$G=\mu_t\left(2\left(\frac{\partial\bar{u}}{\partial x}\right)^2+2\left(\frac{\partial\bar{v}}{\partial r}\right)^2+2\left(\frac{\bar{v}}{r}\right)^2+\left(\frac{\partial\bar{u}}{\partial r}+\frac{\partial\bar{v}}{\partial x}\right)^2\right) \tag{7}$$

and ε-equation

$$\frac{\partial(\rho\varepsilon)}{\partial t}+\frac{\partial(\rho\bar{u}\varepsilon)}{\partial x}+\frac{1}{r}\frac{\partial}{\partial r}(r\rho\bar{v}\varepsilon) = \frac{\partial}{\partial x}\left(\left(\mu+\frac{\mu_t}{\sigma_\varepsilon}\right)\frac{\partial\varepsilon}{\partial x}\right)+\frac{1}{r}\frac{\partial}{\partial r}\left(r\left(\mu+\frac{\mu_t}{\sigma_\varepsilon}\right)\frac{\partial\varepsilon}{\partial r}\right) + C_1 f_1 G\frac{\varepsilon}{k}-C_2 f_2\rho\frac{\varepsilon^2}{k}, \tag{8}$$

where σ_ε is the turbulent Prandtl number for ε, defined as the ratio of the eddy viscosity to the turbulent diffusion coefficient for ε, C_1 and C_2 are the empirical constants of the k–ε model, f_1 and f_2 are the turbulent model functions of the k–ε model, which are

$$\begin{aligned} &C_1=1.4,\quad C_2=1.8,\quad C_\mu=0.09,\\ &\sigma_k=1.4,\quad \sigma_\varepsilon=1.3,\quad \sigma_T=0.95,\\ &f_1=1.0,\\ &f_2=\left(1-\frac{2}{9}\exp\left(-\frac{R_t^2}{36}\right)\right)\left(1-\exp\left(-\frac{y^+}{5}\right)\right)^2,\\ &f_\mu=\left(1+\frac{3.45}{\sqrt{R_t}}\right)\left(1-\exp\left(-\frac{y^+}{70}\right)\right), \end{aligned} \tag{9}$$

where y^+ is the dimensionless distance from the wall, defined as yu_τ/ν. Here u_τ is the wall-friction velocity given by $\sqrt{\tau_w/\rho}$ where τ_w is the wall shear stress.

This LRN turbulent model is based on the eddy viscosity formula Eq. (5), which is valid only in attached shear layers. Therefore, a modification may be needed for separated flows. Fortunately, Seume and Simon [36] have experimentally observed that no flow separation occurred in oscillating turbulent flows. In fact, Ahn and Ibrahim [37] successfully used the standard k–ε model with the help of the wall function method for such an oscillating turbulent flow. Although flow reversal may occur in a pulsating turbulent flow with a large velocity oscillating amplitude, it can be confidently inferred that no flow separation would develop in the pulsating turbulent flow. Consequently, the above mentioned LRN k–ε model can be used for the pulsating turbulent flows with large velocity oscillating amplitudes. It is noted that an LRN k–ε model developed by Launder and Sharma [38] was successfully used by Ismael and Cotton [39] to calculate the wall shear stress in a pulsating turbulent pipe flow.

2.3. Boundary and initial conditions

At the inlet, a parallel uniform flow is assumed and the velocity is considered to be sinusoidally oscillatory around a periodically time-averaged value of the mean velocity. In some cases, for example the flow in pulse combustor, the temperature also pulsates. Here the same wave pattern and the phase angle as those of the inlet velocity are used for the inlet temperature while the no-slip condition at the wall and a constant wall temperature are imposed. At the exit, the velocity and temperature are assumed to be fully developed with zero-velocity gradient and zero-temperature gradient in the axial direction of the pipe because the pipe is long enough. Consequently, the boundary conditions can be formulated as follows:

At $x = 0$,

$$\begin{aligned} &\bar{u}=U(1+A_u\cos(\omega t)),\quad \bar{v}=0,\\ &k=0.01\left(\frac{1}{2}\bar{u}_0^2\right),\quad \varepsilon=C_\mu f_\mu\frac{k^2C}{DU},\\ &\overline{T}=\Theta+A_T(\Theta-T_w)\cos(\omega t), \end{aligned} \tag{10}$$

where U is the periodic time-average of the mean velocity at $x = 0$, A_u is the oscillating amplitude of the inlet velocity, ω is the angular frequency, $\bar{u}_0$ is the inlet velocity, C is constant, D is the pipe diameter, Θ is the periodic time-average of the mean temperature at $x = 0$, A_T is the oscillating amplitude of the inlet temperature, T_w is the wall temperature.

At $x = L$,

$$\frac{\partial\bar{u}}{\partial x}=0,\quad \frac{\partial\bar{v}}{\partial x}=0,\quad \frac{\partial k}{\partial x}=0,\quad \frac{\partial\varepsilon}{\partial x}=0,\quad \frac{\partial\overline{T}}{\partial x}=0. \tag{11}$$

At $r = 0$,

$$\frac{\partial\bar{u}}{\partial r}=0,\quad \bar{v}=0,\quad \frac{\partial k}{\partial r}=0,\quad \frac{\partial\varepsilon}{\partial r}=0,\quad \frac{\partial\overline{T}}{\partial r}=0. \tag{12}$$

At $r = R$,

$$\bar{u}=0,\quad \bar{v}=0,\quad k=0,\quad \varepsilon=2\nu\left(\frac{\partial\sqrt{k}}{\partial r}\right)^2,\quad \overline{T}=T_w. \tag{13}$$

The initial flow velocity is taken as zero and the initial fluid temperature is considered to equal the wall temperature. Therefore, the initial conditions (for $t \leqslant 0$) are written as

$$\begin{aligned} &\bar{u}=0,\quad \bar{v}=0,\quad k=k_0,\quad \varepsilon=\varepsilon_0,\\ &\overline{T}=\Theta\quad (x=0),\\ &\overline{T}=T_w\quad (x>0), \end{aligned} \tag{14}$$

where k_0 and ε_0 are the inlet turbulent kinetic energy and the inlet turbulent energy dissipation rate, respectively.

2.4. Heat transfer coefficients and Nusselt numbers

Due to the unique characteristics of the pulsating flow, several heat transfer coefficients have to be carefully defined. The instantaneous local heat transfer coefficient is defined as

$$h(x,t)=\frac{-K\left.\frac{\partial\overline{T}}{\partial r}\right|_{r=R}}{\overline{T}_{\mathrm{av}}-T_{\mathrm{w}}}, \tag{15}$$

where K is the thermal conductivity, $\overline{T}_{\mathrm{av}}$ is the bulk temperature, which, in general, is defined as the velocity-weighted average of the fluid temperature across the pipe and given by

$$\overline{T}_{\mathrm{av}}(x,t)=\frac{\int_0^R \bar{u}(x,r,t)\overline{T}(x,r,t)r\,\mathrm{d}r}{\int_0^R \bar{u}(x,r,t)r\,\mathrm{d}r}. \tag{16}$$

However, in pulsating flows with large velocity oscillation amplitudes, a flow reversal occurs and consequently, Eq. (16) loses its physical meaning. In this case, the section-average temperature is applied [20,40], which is defined as

$$\overline{T}_{\mathrm{av}}(x,t)=\frac{\int_0^R \overline{T}(x,r,t)r\,\mathrm{d}r}{\int_0^R r\,\mathrm{d}r}. \tag{17}$$

The local heat transfer coefficient, defined as the average of heat transfer coefficient over a cycle, is formulated as

$$h_x(x)=\frac{1}{2\pi}\int_0^{2\pi} h\,\mathrm{d}(\omega t). \tag{18}$$

The instantaneous heat transfer coefficient, defined as the average of heat transfer coefficient over the whole length of pipe at a given moment, is expressed as

$$h_t(t)=\frac{1}{L}\int_0^L h\,\mathrm{d}x. \tag{19}$$

Subsequently, several relevant Nusselt numbers are rationally introduced. The instantaneous local Nusselt number is

$$Nu_{x,t}(x,t)=\frac{hD}{K}. \tag{20}$$

The local Nusselt number is

$$Nu_x(x)=\frac{h_xD}{K}=\frac{1}{2\pi}\int_0^{2\pi} Nu_{x,t}\,\mathrm{d}(\omega t). \tag{21}$$

The instantaneous Nusselt number is

$$Nu_t(t)=\frac{h_tD}{K}=\frac{1}{L}\int_0^L Nu_{x,t}\,\mathrm{d}x. \tag{22}$$

The overall Nusselt number, Nu, can be defined as

$$Nu=\frac{1}{2\pi L}\int_0^L\int_0^{2\pi} Nu_{x,t}\,\mathrm{d}(\omega t)\,\mathrm{d}x, \tag{23}$$

which can be also expressed as

$$Nu=\frac{1}{L}\int_0^L Nu_x\,\mathrm{d}x=\frac{D}{KL}\int_0^L h_x\,\mathrm{d}x \tag{24}$$

or

$$Nu=\frac{1}{2\pi}\int_0^{2\pi} Nu_t\,\mathrm{d}(\omega t)=\frac{D}{2\pi K}\int_0^{2\pi} h_t\,\mathrm{d}(\omega t). \tag{25}$$

It should be noted that due to the flow reversal in pulsating flows with large velocity oscillating amplitudes, the wall shear stress has to be carefully treated, which is defined as

$$\tau_{\mathrm{w}}=\begin{cases}-\mu\dfrac{\partial\bar{u}}{\partial r} & \text{for normal flow,}\\ \mu\dfrac{\partial\bar{u}}{\partial r} & \text{for flow reversal.}\end{cases} \tag{26}$$

2.5. Derivation of dimensionless formulas

The relevant dimensionless parameters are defined as

$$\begin{aligned}&x^*=\frac{x}{R},\quad r^*=\frac{r}{R},\quad t^*=\frac{\omega t}{2\pi},\\ &\bar{u}^*=\frac{\bar{u}}{U},\quad \bar{v}^*=\frac{\bar{v}}{U},\quad \bar{p}^*=\frac{\bar{p}}{\rho U^2},\\ &\overline{T}^*=\frac{\overline{T}-T_{\mathrm{w}}}{\Theta-T_{\mathrm{w}}},\quad k^*=\frac{k}{U^2},\quad \varepsilon^*=\frac{\varepsilon\nu}{U^4}.\end{aligned} \tag{27}$$

Subsequently, the governing equations, the boundary conditions, and the initial conditions are non-dimensionalized using these non-dimensional parameters and expressed as follows. Dimensionless continuity equation is

$$\frac{\partial\bar{u}^*}{\partial x^*}+\frac{1}{r^*}\frac{\partial}{\partial r^*}(r^*\bar{v}^*)=0. \tag{28}$$

Dimensionless momentum equation in x-direction is

$$\begin{aligned}&\frac{Wo^2}{\pi Re}\frac{\partial\bar{u}^*}{\partial t^*}+\frac{\partial(\bar{u}^*\bar{u}^*)}{\partial x^*}+\frac{1}{r^*}\frac{\partial}{\partial r^*}(r^*\bar{v}^*\bar{u}^*)\\ &\quad=-\frac{\partial\bar{p}^*}{\partial x^*}+\frac{\partial}{\partial x^*}\left(\frac{2}{Re}\left(1+C_\mu f_\mu\frac{k^{*2}}{\varepsilon^*}\right)\frac{\partial\bar{u}^*}{\partial x^*}\right)\\ &\qquad+\frac{1}{r^*}\frac{\partial}{\partial r^*}\left(r^*\frac{2}{Re}\left(1+C_\mu f_\mu\frac{k^{*2}}{\varepsilon^*}\right)\frac{\partial\bar{u}^*}{\partial r^*}\right)\\ &\qquad+\frac{\partial}{\partial x^*}\left(\frac{2}{Re}\left(1+C_\mu f_\mu\frac{k^{*2}}{\varepsilon^*}\right)\frac{\partial\bar{u}^*}{\partial x^*}\right)\\ &\qquad+\frac{1}{r^*}\frac{\partial}{\partial r^*}\left(r^*\frac{2}{Re}\left(1+C_\mu f_\mu\frac{k^{*2}}{\varepsilon^*}\right)\frac{\partial\bar{v}^*}{\partial x^*}\right),\end{aligned} \tag{29}$$

where $Wo=R\sqrt{\omega/\nu}$ is the Womersley number, $Re=UD/\nu$ is the Reynolds number.

Dimensionless momentum equation in r-direction is

$$\begin{aligned}&\frac{Wo^2}{\pi Re}\frac{\partial\bar{v}^*}{\partial t^*}+\frac{\partial(\bar{u}^*\bar{v}^*)}{\partial x^*}+\frac{1}{r^*}\frac{\partial}{\partial r^*}(r^*\bar{v}^*\bar{v}^*)\\ &\quad=-\frac{\partial\bar{p}^*}{\partial r^*}+\frac{\partial}{\partial x^*}\left(\frac{2}{Re}\left(1+C_\mu f_\mu\frac{k^{*2}}{\varepsilon^*}\right)\frac{\partial\bar{v}^*}{\partial x^*}\right)\\ &\qquad+\frac{1}{r^*}\frac{\partial}{\partial r^*}\left(r^*\frac{2}{Re}\left(1+C_\mu f_\mu\frac{k^{*2}}{\varepsilon^*}\right)\frac{\partial\bar{v}^*}{\partial r^*}\right)\\ &\qquad+\frac{\partial}{\partial x^*}\left(\frac{2}{Re}\left(1+C_\mu f_\mu\frac{k^{*2}}{\varepsilon^*}\right)\frac{\partial\bar{u}^*}{\partial r^*}\right)\\ &\qquad+\frac{1}{r^*}\frac{\partial}{\partial r^*}\left(r^*\frac{2}{Re}\left(1+C_\mu f_\mu\frac{k^{*2}}{\varepsilon^*}\right)\frac{\partial\bar{v}^*}{\partial r^*}\right)\\ &\qquad-\frac{2}{Re}\left(1+C_\mu f_\mu\frac{k^{*2}}{\varepsilon^*}\right)\frac{2\bar{v}^*}{r^{*2}}.\end{aligned} \tag{30}$$

Dimensionless k-equation is

$$\frac{Wo^2}{\pi Re}\frac{\partial k^*}{\partial t^*}+\frac{\partial(\bar{u}^*k^*)}{\partial x^*}+\frac{1}{r^*}\frac{\partial}{\partial r^*}(r^*\bar{v}^*k^*) = \frac{\partial}{\partial x^*}\left(\frac{2}{Re}\left(1+C_\mu f_\mu\frac{k^{*2}}{\varepsilon^*\sigma_k}\right)\frac{\partial k^*}{\partial x^*}\right) + \frac{1}{r^*}\frac{\partial}{\partial r^*}\left(r^*\frac{2}{Re}\left(1+C_\mu f_\mu\frac{k^{*2}}{\varepsilon^*\sigma_k}\right)\frac{\partial k^*}{\partial r^*}\right) + \frac{2}{Re}C_\mu f_\mu\frac{k^{*2}}{\varepsilon^*}G^*-\frac{Re}{2}\varepsilon^*, \tag{31}$$

where

$$G^*=\left(2\left(\frac{\partial\bar{u}^*}{\partial x^*}\right)^2+2\left(\frac{\partial\bar{v}^*}{\partial r^*}\right)^2+2\left(\frac{\bar{v}^*}{r^*}\right)^2+\left(\frac{\partial\bar{u}^*}{\partial r^*}+\frac{\partial\bar{v}^*}{\partial x^*}\right)^2\right). \tag{32}$$

Dimensionless ε-equation is

$$\frac{Wo^2}{\pi Re}\frac{\partial \varepsilon^*}{\partial t^*}+\frac{\partial(\bar{u}^*\varepsilon^*)}{\partial x^*}+\frac{1}{r^*}\frac{\partial}{\partial r^*}(r^*\bar{v}^*\varepsilon^*) = \frac{\partial}{\partial x^*}\left(\frac{2}{Re}\left(1+C_\mu f_\mu\frac{k^{*2}}{\varepsilon^*\sigma_\varepsilon}\right)\frac{\partial \varepsilon^*}{\partial x^*}\right) + \frac{1}{r^*}\frac{\partial}{\partial r^*}\left(r^*\frac{2}{Re}\left(1+C_\mu f_\mu\frac{k^{*2}}{\varepsilon^*\sigma_\varepsilon}\right)\frac{\partial \varepsilon^*}{\partial r^*}\right) + \frac{2}{Re}C_\mu f_\mu k^* C_1 f_1 G^*-\frac{Re}{2}C_2 f_2\frac{\varepsilon^{*2}}{k^*}. \tag{33}$$

Dimensionless energy equation is

$$\frac{Wo^2}{\pi Re}\frac{\partial \overline{T}^*}{\partial t^*}+\frac{\partial(\bar{u}^*\overline{T}^*)}{\partial x^*}+\frac{1}{r^*}\frac{\partial}{\partial r^*}(r^*\bar{v}^*\overline{T}^*) = \frac{\partial}{\partial x^*}\left(\frac{2}{Re}\left(\frac{1}{Pr}+C_\mu f_\mu\frac{k^{*2}}{\varepsilon^*\sigma_T}\right)\frac{\partial \overline{T}^*}{\partial x^*}\right) + \frac{1}{r^*}\frac{\partial}{\partial r^*}\left(r^*\frac{2}{Re}\left(\frac{1}{Pr}+C_\mu f_\mu\frac{k^{*2}}{\varepsilon^*\sigma_T}\right)\frac{\partial \overline{T}^*}{\partial r^*}\right). \tag{34}$$

It can be found that, besides Reynolds number and Prandtl number, Womersley number is also an important parameter in the study of pulsating flow. In fact, relative to oscillating frequency, Womersley number is more qualified to represent the characteristics of pulsating flow.

The corresponding dimensionless boundary conditions are:

at $x^*=0$,

$$\bar{u}^*=1+A_u\cos(2\pi t^*),\quad \bar{v}^*=0,\quad k^*=0.01\left(\frac{1}{2}\bar{u}_0^{*2}\right),$$
$$\varepsilon^*=C_\mu f_\mu\frac{k^{*2}C}{Re},\quad \overline{T}^*=1+A_T\cos(2\pi t^*) \tag{35}$$

at $x^*=L/R$,

$$\frac{\partial\bar{u}^*}{\partial x^*}=0,\quad \frac{\partial\bar{v}^*}{\partial x^*}=0,\quad \frac{\partial k^*}{\partial x^*}=0,$$
$$\frac{\partial\varepsilon^*}{\partial x^*}=0,\quad \frac{\partial\overline{T}^*}{\partial x^*}=0 \tag{36}$$

at $r^*=0$,

$$\frac{\partial\bar{u}^*}{\partial r^*}=0,\quad \bar{v}^*=0,\quad \frac{\partial k^*}{\partial r^*}=0,$$
$$\frac{\partial\varepsilon^*}{\partial r^*}=0,\quad \frac{\partial\overline{T}^*}{\partial r^*}=0 \tag{37}$$

at $r^*=1$,

$$\bar{u}^*=0,\quad \bar{v}^*=0,\quad k^*=0,$$
$$\varepsilon^*=\frac{8}{Re^2}\left(\frac{\partial\sqrt{k^*}}{\partial r^*}\right)^2,\quad \overline{T}^*=0. \tag{38}$$

The dimensionless initial conditions are:

$$\bar{u}^*=0,\quad \bar{v}^*=0,\quad k^*=k_0^*,\quad \varepsilon^*=\varepsilon_0^*,$$
$$\overline{T}^*=1\quad (x^*=0),$$
$$\overline{T}^*=0\quad (x^*>0). \tag{39}$$

The corresponding dimensionless expressions of the relevant heat transfer coefficients and Nusselt numbers are given by

$$h(x^*,t^*)=-\frac{K}{R\overline{T}^*_{\mathrm{av}}}\left.\frac{\partial\overline{T}^*}{\partial r^*}\right|_{r^*=1}, \tag{40}$$

where

$$\overline{T}^*_{\mathrm{av}}(x^*,t^*)=\frac{\int_0^1\overline{T}^*(x^*,r^*,t^*)r^*\,\mathrm{d}r^*}{\int_0^1 r^*\,\mathrm{d}r^*}, \tag{41}$$

$$h_x(x^*)=\int_0^1 h\,\mathrm{d}t^*=-\frac{K}{R}\int_0^1\frac{1}{\overline{T}^*_{\mathrm{av}}}\left.\frac{\partial\overline{T}^*}{\partial r^*}\right|_{r^*=1}\mathrm{d}t^*, \tag{42}$$

$$h_t(t^*)=\frac{1}{L^*}\int_0^{L^*}h\,\mathrm{d}x^*=-\frac{K}{L}\int_0^{L^*}\frac{1}{\overline{T}^*_{\mathrm{av}}}\left.\frac{\partial\overline{T}^*}{\partial r^*}\right|_{r^*=1}\mathrm{d}x^*, \tag{43}$$

$$Nu_x(x^*)=\frac{h_xD}{K}=-2\int_0^1\frac{1}{\overline{T}^*_{\mathrm{av}}}\left.\frac{\partial\overline{T}^*}{\partial r^*}\right|_{r^*=1}\mathrm{d}t^*, \tag{44}$$

$$Nu_t(t^*)=\frac{h_tD}{K}=-\frac{2}{L^*}\int_0^{L^*}\frac{1}{\overline{T}^*_{\mathrm{av}}}\left.\frac{\partial\overline{T}^*}{\partial r^*}\right|_{r^*=1}\mathrm{d}x^*, \tag{45}$$

$$Nu=\frac{D}{KL}\int_0^L h_x\,\mathrm{d}x=-\frac{2}{L^*}\int_0^{L^*}\int_0^1\frac{1}{\overline{T}^*_{\mathrm{av}}}\left.\frac{\partial\overline{T}^*}{\partial r^*}\right|_{r^*=1}\mathrm{d}t^*\,\mathrm{d}x^*. \tag{46}$$

The denotation of time-average value, "–", is omitted hereafter for simplicity.

2.6. Numerical model

The discretization of the governing differential equations is performed using the finite volume method [41] applied to a staggered orthogonal grid system. A power-law scheme is employed for convection fluxes. The SIMPLEC algorithm [41,42], which is a powerful algorithm to solve fluid flow and heat transfer problems, is used and the discretized equations are solved with the

line-by-line ADI (Alternating-Direction Implicit) iterative method. The solution of each point at each grid line is directly obtained through the TDMA (TriDiagonal Matrix Algorithm). To accelerate convergence, a recommended value 1.85 of the relaxation parameter is introduced in the TDMA solver [42]. The convergence criteria with Euclidean norm of the residuals are used in solving the governing equations in each cycle of iteration [42]. Meanwhile, under-relaxation is applied for the momentum equations, k-equation, and ε-equation.

2.7. Verification of computer code for pulsating turbulent flows

To verify the correctness of the computer code for the calculation of heat transfer in pulsating turbulent flow, a comparison between the present numerical results and available experimental data is made first. Since experimental data in pulsating turbulent flow with large oscillating velocity amplitudes is lacking, experimental results obtained by Tu and Ramaprian [5] are used as the comparison data. Tu and Ramaprian experimentally measured the sectional velocity distribution in the fully developed pulsating turbulent flow of water, in which the Reynolds number was $Re = 50{,}000$ and the Womersley number was $Wo = 118.5$. Although the oscillating velocity amplitude A_u was only 0.15 and consequently no flow reversal occurred, it is still worthy to be used for the examination of our computer code for the calculation of the pulsating turbulent flow in a pipe. Both numerical and experimental sectional velocities of fully developed pulsating turbulent pipe flow are shown in Fig. 2(a). They agree well with each other, indicating that our computer code is practically usable for the computation of pulsating turbulent flow.

The computation results are also compared with the experimental results obtained by Fallen [21]. In his experiment, water was used as the medium of heat transfer, Reynolds number was between 1000 and 107,000, the oscillating frequency was from 0.5 to 4 cycles per second, and the oscillating velocity amplitude was up to 4. The comparison between the numerical and the experimental results for the heat transfer enhancement is displayed in Fig. 2(b). It can be seen that the numerical data fall inside the limits of the experimental data, demonstrating the dependability of our computer code for the computation of the heat transfer in the pulsating turbulent flow.

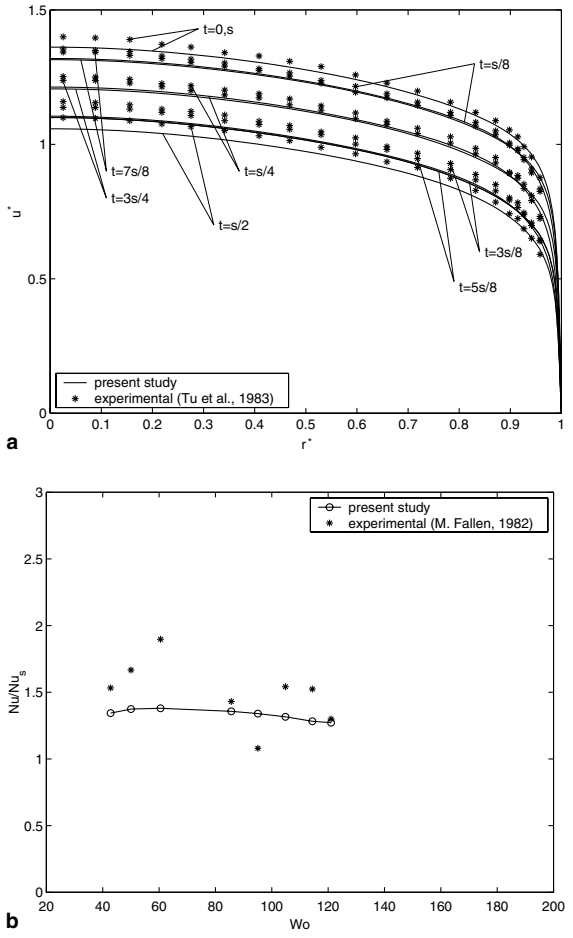

Fig. 2. Verification of computer code: (a) sectional velocity in fully developed pulsating turbulent flow in a period with $Re = 50{,}000$, $Wo = 118.5$, $A_u = 0.15$ and (b) heat transfer enhancement in pulsating turbulent flow with $Re = 35{,}000$, $A_u = 2$.

3. Results and discussion

3.1. Steady state turbulent flow and heat transfer

First of all, numerical study on heat transfer in steady state turbulent pipe flow with $Re = 25{,}000$ and $Pr = 0.703$ is conducted to examine the computer code. In the present study, very fine grids are deployed near the wall regions. About 15 control volumes are taken within $y^+ < 10$. In order to eliminate the effect of grid size on the calculation results, several cases of heat transfer in steady state turbulent pipe flow with different grid sizes are checked. As is well known, the fully developed turbulent flow is formed at about $L/D = 10-60$ [43,44] in a pipe. Here the Nusselt number at $x^* = 160$ (corresponding to $L/D = 80$) is chosen as the Nusselt number of fully developed turbulent flow. The Nusselt number of fully developed turbulent flow in a pipe can be also determined from the correlation obtained by Petukhov and Popov [45,46]

$$Nu_{\mathrm{corl}} = \frac{(f/2)RePr}{(1+13.6f)+(11.7+1.8Pr^{-1/3})(f/2)^{1/2}(Pr^{2/3}-1)}, \tag{47}$$

where

$$f = (3.64 \log Re - 3.28)^{-2}. \quad (48)$$

For $Re = 25{,}000$ and $Pr = 0.703$, the exact value of Nusselt number is 58.68. Table 1 shows the test results of grid independence. The relative error of numerically calculated Nusselt number at $x^* = 160$ to the value from Eq. (47), γ, is evaluated for different grid sizes and listed in Table 1, which are within a reasonable tolerance range. It can be seen that the grid size 280×72 (axial $\times$ radial) is good enough for the present numerical calculations and the chosen domain length $L/R = 200$ is long enough to keep the flow hydrodynamically and thermally fully developed.

3.2. The effect of temperature oscillation at inlet

Similar to the velocity boundary condition at inlet, the temperature boundary condition at the inlet is also set to oscillate sinusoidally around a periodically time-averaged temperature with the same phase as velocity. Table 2 gives the test results for several cases with different values of temperature oscillation amplitude A_T. It is shown that the heat transfer is hardly affected by the temperature oscillation amplitude. Therefore, it is reasonable to take $A_T = 0.02$ in the present study.

3.3. Cyclic axial velocity, temperature, and pressure at centerline

Fig. 3 shows cyclic centerline velocities u_c^* and temperatures T_c^* in the fully developed region with $Re = 25{,}000$ and $A_u = 3$ for different Womersley numbers. It can be seen that the velocity always pulsates sinusoidally, corresponding to the pulsating form of the inlet velocity. The two zero-velocity crosspoints indicate the streamwise velocity goes through zero twice in each cycle, one passes through zero from positive at about $t^* = 0.3$ and the other passes through zero from negative at about $t^* = 0.7$. That means a flow reversal occurs in each pulsating period.

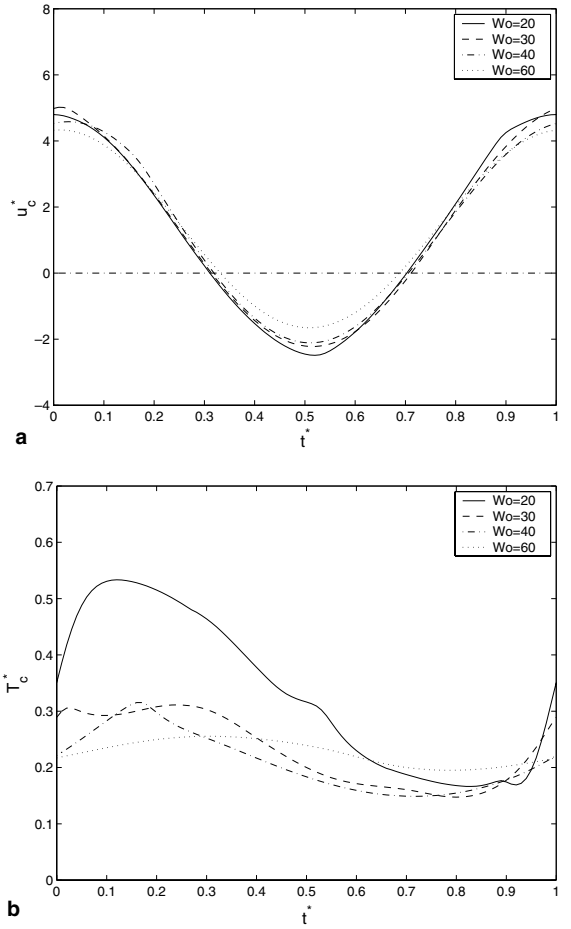

Fig. 3. Cyclic velocity and temperature at centerline for $Re = 25{,}000$, $A_u = 3$: (a) cyclic velocity and (b) cyclic temperature.

Table 1
Tests on grid independence ($Re = 25{,}000$, $Pr = 0.703$)

Grid (axial × radial)	Nu_s	$Nu_{x,s}(x^* = 160)$	γ (%)
180×62	72.87	63.73	8.6
280×62	68.55	63.43	8.1
280×72	67.85	61.30	4.5
280×82	69.57	60.97	3.9
380×72	66.20	61.00	4.0
380×82	66.83	60.82	3.6

Table 2
The effect of temperature oscillation at inlet on heat transfer ($Re = 25{,}000$, $Pr = 0.703$, $Wo = 40$, $A_u = 3$)

A_T	Nu	$Nu_x(x^* = 160)$
0.01	106.6040	98.1718
0.02	106.6031	98.1715
0.1	106.5963	98.1696
0.2	106.5891	98.1675

The cyclic temperatures at the centerline for different Womersley numbers display non-sinusoidal curves except the case of $Wo = 60$, as shown in Fig. 3(b). It is obvious that the distortion of the cyclic temperature curves deviated from the sinusoidal fluctuation damps with the increase in the Womersley number. Similar cyclic centerline velocity and temperature pulsations were found in experimental results of turbulent pulsating channel flow with large velocity oscillating amplitudes by Dec et al. [20,47,48].

The cyclic pressure at the centerline p_c^* is shown in Fig. 4(a). It is sinusoidal, which is in accord with the pulsation pattern of velocity but with a phase lag. Fig. 4(b)

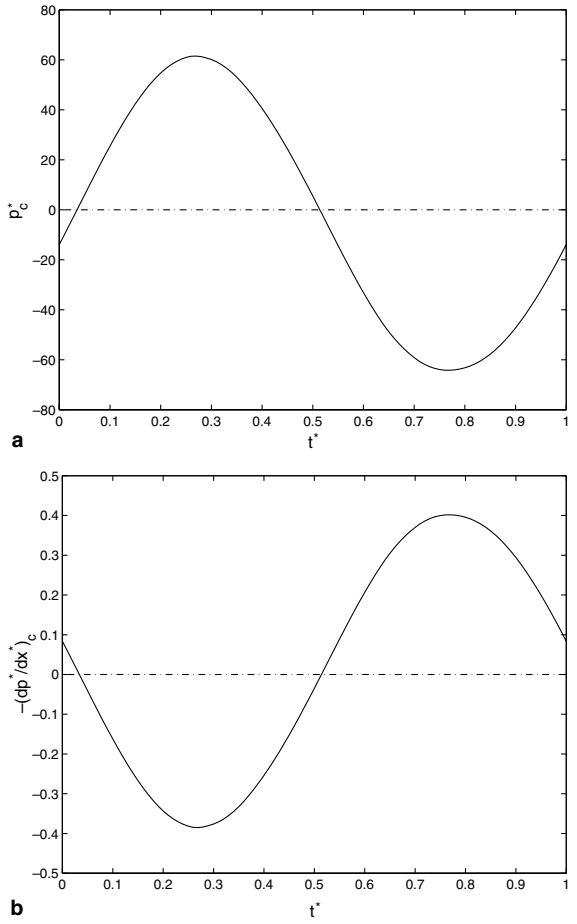

Fig. 4. Cyclic pressure and axial pressure gradient at centerline for $Re = 25{,}000$, $Wo = 40$, $A_u = 3$: (a) cyclic pressure and (b) cyclic pressure gradient.

shows cyclic axial pressure gradient at the centerline, $(dp^*/dx^*)_c$, which is also sinusoidal. Comparing the phase of velocity in Fig. 3(a) and that of axial pressure gradient, about 90° phase lag of the axial pressure gradient to the velocity is found. This result agrees with earlier analytical solution for pulsating laminar flow obtained by Uchida [49]. According to the analytical solution, out-of-phase between velocity and axial pressure gradient occurs and approaches 90° at a high Womersley number. Since the pressure gradient changes periodically from favorable to adverse, it results in periodic flow reversal when the velocity oscillation amplitude becomes larger.

3.4. Time-resolved sectional axial velocity and temperature in a period

Because the velocity and the temperature in pulsating flow change periodically, understanding the characteristics of the flow and the temperature at different times within a cycle, i.e., so-called time-resolved velocity and temperature, is important to the study. The fully developed sectional time-resolved velocity during a period is shown in Fig. 5(a). The velocity varies from positive to negative and vice versa during a period due to the large velocity oscillatory amplitude and the change of the pressure gradient. In the great portion of the pipe section around the center of pipe, the velocity profile is flat. This region can be named as the core region. Near the wall, the velocity gradient becomes very large, corresponding to the boundary layer and is called the boundary region. In the buffer region between the core and the boundary regions, a velocity "overshoot" occurs at a few moments, for example, at $t^* = 0.3$, 0.4, 0.7, and 0.8, shown in Fig. 5(a). That means the flow velocity at these moments exceeds the velocity in the core region and, hence, causes larger velocity gradient at the wall than that in steady-state flow. Consequently, more heat is transported at these moments. This phenomenon is also called Richardson effect [49]. It happens when the streamwise velocity passes through the zero-velocity crosspoints. Obviously, flow reversal greatly affects the heat transfer enhancement in pulsating turbulent flow. As is well known, the Richardson effect also exists in pulsating laminar flow. However, the buffer region in pulsating turbulent flow is much larger than one in pulsating laminar flow.

Fig. 5(b) and (c) are the time-resolved sectional temperature in a period for fully developed pulsating flow. In the pipe center region, the temperature profile is flat, while at the region near the wall, the temperature gradient becomes very large, corresponding to the thermal boundary layer. The thickness of the thermal boundary layer varies with the pulsation of fluid flow in the period. Unlike the velocity profile, there is no Richardson effect in the temperature profile. The fully developed sectional temperature in steady state pipe flow is also shown in Fig. 5(b) and (c). It can be seen that during a period, the thickness of the thermal boundary in the pulsating flow is sometimes thinner and sometimes thicker than that in steady state flow.

3.5. Nusselt number

The local Nusselt numbers for different Womersley numbers under the conditions of $Re = 25{,}000$ and $A_u = 3$ are plotted in Fig. 6, showing the similar course of curve to the case of steady state pipe flow at the same Reynolds number. At the downstream of the pipe, the curves become flat up to the end, for the flows are fully developed. It can be seen clearly that the heat transfer in a pipe flow is greatly enhanced throughout the pipe by the pulsation. Additionally, for the cases of large Womersley numbers, the curves of the local Nusselt number of the pulsating flows become flat earlier than

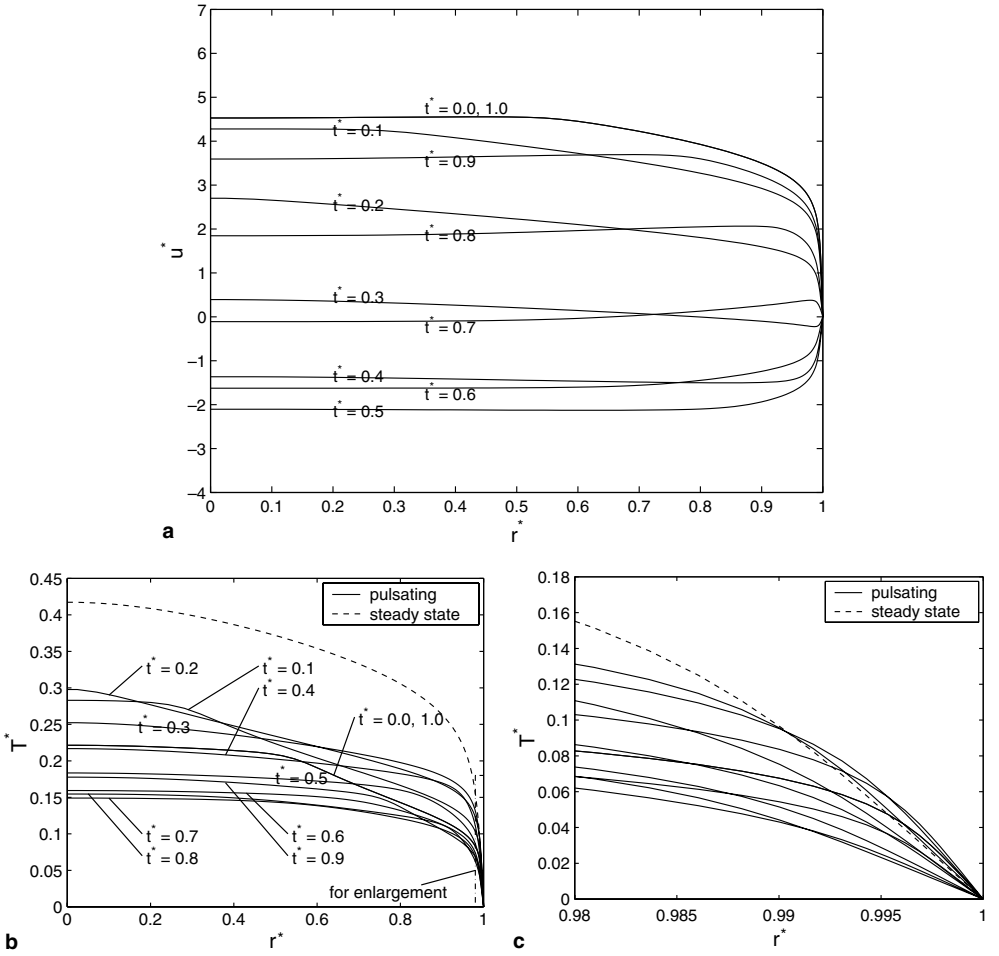

Fig. 5. Sectional velocity and temperature in a period for $Re = 25{,}000$, $Wo = 40$, $A_u = 3$: (a) sectional velocity, (b) sectional temperature, and (c) enlargement of part of sectional temperature.

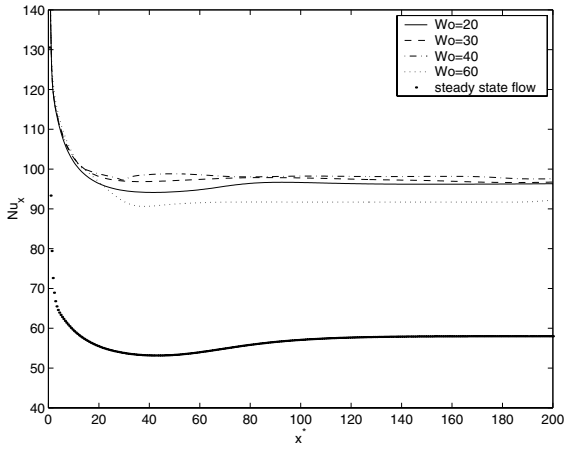

Fig. 6. Local Nusselt number at different Womersley numbers under the conditions of $Re = 25{,}000$, $A_u = 3$.

that of the steady state flow, implying that the pulsating turbulent flows become fully developed with shorter entrance regions. For example, in the case of $Wo = 60$ the entrance region is about $x^* = 60$, which is much shorter than one in the case of steady state flow ($x^* \sim 100$). Comparing the local Nusselt numbers for the cases of $Wo = 40$ and $Wo = 60$, it is found that the curve for $Wo = 60$ is over that for $Wo = 40$ only in the entrance region and soon becomes lower than that for $Wo = 40$ in most part of the pipe. It implies that higher Womersley number benefits to heat transfer enhancement only in the entrance region. It is also seen that to blindly increase in Womersley number can not reach the maximization of the enhancement of heat transfer, instead, an optimal value of Womersley number exists for the heat transfer enhancement, which is found to roughly equal 40.

Fig. 7 shows instantaneous local Nusselt number at fully developed region in a period. Obviously, the

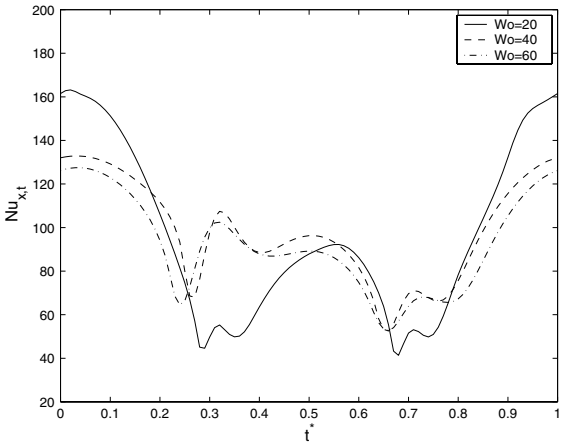

Fig. 7. Instantaneous local Nusselt number in a period at different Womersley numbers under the conditions of $Re = 25{,}000$, $A_u = 3$.

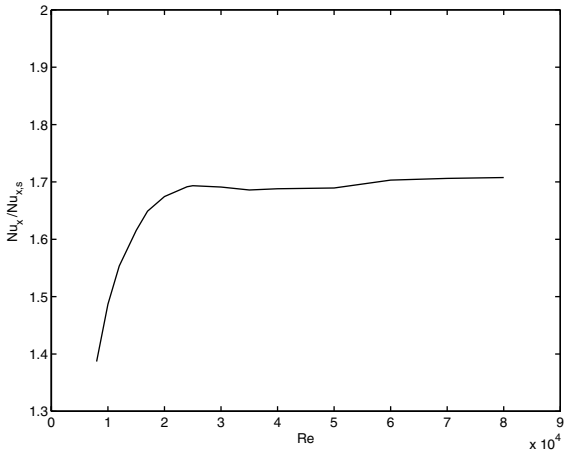

Fig. 8. Heat transfer enhancement for different Reynolds numbers under the conditions of $Wo = 40$, $A_u = 3$.

instantaneous local Nusselt number is non-sinusoidal. Around $t^* = 0$ and $t^* = 1$, the Nusselt number reaches maximum. From Fig. 3(a), it is seen that the flow velocity reaches maximum also at these moments. It indicates that larger velocity induced by pulsation of the fluid flow results in higher heat transfer rate. In the middle of the period, the instantaneous local Nusselt numbers become lower, corresponding to the negative velocities where the flow reverses. While the velocity decreases to the minimum at $t^* = 0.5$, the Nusselt number reaches a local maximum value at or after a little from $t^* = 0.5$. It should be also noted that there are two dips in the curves of the instantaneous local Nusselt number, which coincide with the two zero-velocity crosspoints in the period, respectively. After the velocity passes through the first zero-velocity crosspoint, the flow reversal occurs and Nusselt number increases and then decreases until the velocity approaches the second zero-velocity crosspoint. After the velocity passes through the second zero-velocity crosspoint, Nusselt number increases with the velocity. This clearly reveals that the flow reversal enhances heat transfer. The phases of the two dips in the curve of instantaneous local Nusselt number do not exactly coincide with the phases of the two zero-velocity crosspoints in the curve of the centerline velocity because of the phase lag between the flow reversals at the flow centerline and at the wall.

It is found that Reynolds number strongly affects the heat transfer enhancement denoted by $Nu_x/Nu_{x,s}$, where $Nu_{x,s}$ is the local Nusselt number of steady state turbulent pipe flow. When the Reynolds number is relatively low, the effect of Reynolds number on the heat transfer enhancement in the pulsating turbulent flow sharply increases with Reynolds number. However, when Reynolds number exceeds a certain value, say 2×10^4 for the case of $Wo = 40$ and $A_u = 3$, the effect becomes nearly constant, as shown in Fig. 8. The velocity oscillation amplitude also strongly affects the heat transfer enhancement in the pulsating turbulent flow. When the velocity oscillation amplitude is small, the heat transfer is moderately enhanced, while the enhancement is rapidly increased when the velocity oscillation amplitude exceeds a certain value, say $A_u > 1.5$ for the case of $Re = 25{,}000$ and $Wo = 40$, as shown in Fig. 9. This result well coincides with the experimental results in Ref. [25], where heat transfer enhancement is increased rapidly when $A_u > 1.5$ and heat transfer is not changed when $A_u < 1.5$. The numerical simulation reveals that Womersley number has a complex effect on the heat transfer enhancement. Different from the pulsating laminar flow in which heat transfer is reduced at very small Womersley numbers and enhanced at larger Womersley

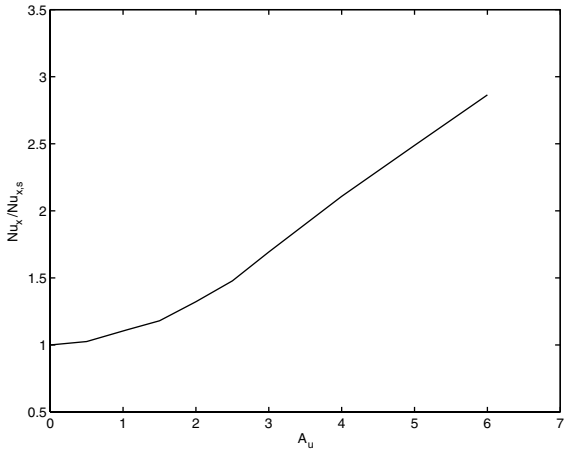

Fig. 9. The effect of velocity oscillating amplitude on heat transfer enhancement for $Re = 25{,}000$, $Wo = 40$.

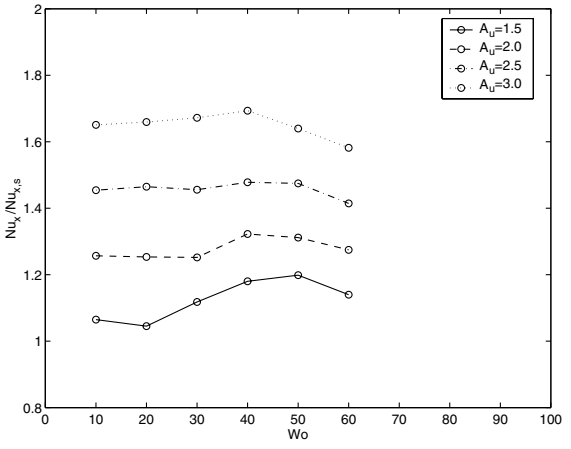

Fig. 10. The effect of Womersley number on heat transfer enhancement for $Re = 25{,}000$.

numbers, the heat transfer in the pulsating turbulent flow is always enhanced by the flow fluctuations, as shown in Fig. 10. It is also discovered that for all different tested oscillation amplitudes of the velocity, an optimal value of Womersley number for the heat transfer enhancement exists between 40 and 50 when Reynolds number is 25,000.

4. Conclusions

A two-dimensional model to describe heat transfer in pulsating turbulent flow in a pipe is developed and simulated with the finite volume method. The simulation results on the fully developed pulsating turbulent flow and the heat transfer enhancement are consistent with the available experimental data. The model analysis shows that Womersley number is an important parameter in the study of pulsating flow and heat transfer.

The numerical results show that pulsating flows with large Womersley numbers become fully developed with shorter entrance region compared with the steady state flow. The heat transfer enhancement is mainly affected by Womersley number and velocity oscillation amplitude. An optimal Womersley number exists and is found to be 40–50 for different velocity oscillating amplitudes at Reynolds number of 25,000. The velocity oscillation amplitude is found to strongly enhance heat transfer, especially when the amplitude exceeds a certain value. The heat transfer enhancement is also affected by Reynolds number, especially at lower Reynolds numbers. Temperature fluctuations at inlet caused by velocity oscillation has no effect on the heat transfer enhancement.

The analysis demonstrates that larger velocity at some moments and the flow reversal during a period of the flow pulsation are the most important mechanism of the heat transfer enhancement.

References

[1] J.H. Gerrard, An experimental investigation of pulsating turbulent water flow in a tube, J. Fluid Mech. 46 (part 1) (1971) 43–64.
[2] T. Mizushina, T. Maruyama, Y. Shiozaki, Pulsating turbulent flow in a tube, J. Chem. Eng. Jpn. 6 (6) (1973) 487–494.
[3] T. Mizushina, T. Maruyama, H. Hirasawa, Structure of the turbulence in pulsating pipe flows, J. Chem. Eng. Jpn. 8 (3) (1975) 210–216.
[4] R.E. Kirmse, Investigations of pulsating turbulent pipe flow, Trans. ASME, J. Fluids Eng. 101 (4) (1979) 436–442.
[5] S.W. Tu, B.R. Ramaprian, Fully developed periodic turbulent pipe flow, Part 1. Main experimental results and comparison with predictions, J. Fluid Mech. 137 (1983) 31–58.
[6] L. Shemer, I. Wygnanski, E. Kit, Pulsating flow in a pipe, J. Fluid Mech. 153 (1985) 313–337.
[7] Z.-X. Mao, T.J. Hanratty, Studies of the wall shear stress in a turbulent pulsating pipe flow, J. Fluid Mech. 170 (1986) 545–564.
[8] S. Isshiki, T. Obata, N. Kasagi, M. Hirata, Experimental study on heat transfer in a pulsating pipe flow, Trans. JSME, Part B 59 (563) (1993) 145–151.
[9] S. Isshiki, T. Obata, N. Kasagi, M. Hirata, Experimental study on heat transfer in a pulsating pipe flow (2nd report, phase-averaged turbulent characteristics), Trans. JSME, Part B 59 (564) (1993) 2522–2528.
[10] S.F. Tardu, G. Binder, R.F. Blackwelder, Turbulent channel flow with large-amplitude velocity oscillations, J. Fluid Mech. 267 (1994) 109–151.
[11] R.C. Martinelli, L.M.K. Boelter, E.B. Weinberg, S. Yakahi, Heat transfer to a fluid flowing periodically at low frequencies in a vertical tube, Trans. ASME 65 (7) (1943) 789–798.
[12] L.G. Genin, A.P. Koval, S.P. Manchkha, V.G. Sviridov, Heat transfer and friction for pulsating water flow in a pipe, Heat Transfer Res. 25 (2) (1993) 192–195.
[13] A.R. Barker, J.E.F. Williams, Transient measurements of the heat transfer coefficient in unsteady, turbulent pipe flow, Int. J. Heat Mass Transfer 43 (2000) 3197–3207.
[14] J.S. Park, M.F. Taylor, D.M. McEligot, Heat transfer to pulsating, turbulent gas flow, in: Proceedings of the 7th International Heat Transfer Conference, vol. 3, 1982, pp. 105–110.
[15] H.A. Havemann, N.N.N. Rao, Heat transfer in pulsating flow, Nature 174 (1954) 41.
[16] N.-S. Liao, C.-C. Wang, On the convective heat transfer in pulsating turbulent pipe flow, in: R.K. Shah, E.N. Ganic, K.T. Yang (Eds.), Experimental Heat Transfer, Fluid Mechanics, and Thermodynamics, Elsevier Science Publishing Co., Inc., 1988, pp. 536–542.
[17] O.E. Karamercan, J.L. Gainer, The effect of pulsations on heat transfer, Ind. Eng. Chem. Fundam. 18 (1) (1979) 11–15.

[18] F.B. West, A.T. Taylor, The effect of pulsations on heat transfer (turbulent flow of water inside tubes), Chem. Eng. Progress 48 (1) (1952) 39–43.
[19] R. Lemlich, Vibration and pulsation boost heat transfer, Chem. Eng. 68 (10) (1961) 171–176.
[20] J.E. Dec, J.O. Keller, V.S. Arpaci, Heat transfer enhancement in the oscillating turbulent flow of a pulse combustor tail pipe, Int. J. Heat Mass Transfer 35 (9) (1992) 2311–2325.
[21] K.M. Fallen, Heat transfer in a pipe with superimposed pulsating flow, Warme Stoffubertragung (Thermo-Fluid Dyn.) 16 (1982) 89–99.
[22] S.A. Gbadebo, S.A.M. Said, M.A. Habib, Average Nusselt number correlation in the thermal entrance region of steady and pulsating turbulent pipe flows, Heat Mass Transfer (Warme Stoffubertragung) 35 (5) (1999) 377–381.
[23] A.A. AI-Haddad, N. AI-Binally, Prediction of heat transfer coefficient in pulsating flow, Int. J. Heat Fluid Flow 10 (2) (1989) 131–133.
[24] M.H.I. Baird, G.J. Duncan, J.I. Smith, J. Taylor, Heat transfer in pulsed turbulent flow, Chem. Eng. Sci. 21 (2) (1966) 197–199.
[25] R.H. Keil, M.H.I. Baird, Enhancement of heat transfer by flow pulsation, Ind. Eng. Chem. Process. Des. Develop. 10 (4) (1971) 473–478.
[26] J.C. Ludlow, D.J. Kirwan, J.L. Gainer, Heat transfer with pulsating flow, Chem. Eng. Commun. 7 (1980) 211–218.
[27] P. Andre, R. Creff, J. Batina, Numerical study in heat transfer for a turbulent pulsed ducted flow, Numer. Heat Transfer 9 (1986) 201–216.
[28] E.P. Valueva, V.N. Popov, Mathematical modeling of the pulsating turbulent flow of a liquid in a circular tube, Phys. Dokl. 38 (9) (1993) 359–362.
[29] E.P. Valueva, V.N. Popov, S.Y. Romanova, Heat transfer in pulsating turbulent flow in a round tube, Thermal Eng. 41 (3) (1994) 182–193.
[30] S. Thyageswaran, Numerical modeling of pulse combustor tail pipe heat transfer, Int. J. Heat Mass Transfer 47 (2004) 2637–2651.
[31] A. Scotti, U. Piomelli, Turbulence models in pulsating flows, AIAA J. 40 (3) (2002) 537–544.
[32] W.P. Jones, B.E. Launder, The prediction of laminarization with a two-equation model of turbulence, Int. J. Heat Mass Transfer 15 (2) (1972) 301–314.
[33] W.P. Jones, B.E. Launder, The calculation of low-Reynolds-number phenomena with a two-equation model of turbulence, Int. J. Heat Mass Transfer 16 (1973) 1119–1130.
[34] V.C. Patel, W. Rodi, G. Scheuerer, Turbulence models for near-wall and low Reynolds number flows: a review, AIAA J. 23 (9) (1985) 1308–1319.
[35] S. Torii, W.-J. Yang, Thermal transport in turbulent couette flows in concentric annuli for various Prandtl numbers, Numer. Heat Transfer, Part A 34 (1998) 537–552.
[36] J.R. Seume, T.W. Simon, Oscillating flow in Stirling engine heat exchangers, in: Proceedings of the 21st Intersociety Energy Conversion Engineering Conference, IECEC, San Diego, CA, 1986, pp. 533–538.
[37] K.H. Ahn, M.B. Ibrahim, Laminar/turbulent oscillating flow in circular pipes, Int. J. Heat Fluid Flow 13 (4) (1992) 340–346.
[38] B.E. Launder, B.I. Sharma, Application of the energy dissipation model of turbulence to the calculation of flow near a spinning disc, Lett. Heat Mass Transfer 1 (1974) 131–138.
[39] J.O. Ismael, M.A. Cotton, Calculations of wall shear stress in harmonically oscillated turbulent pipe flow using a low-Reynolds-number k–ε model, Trans. ASME, J. Fluids Eng. 118 (1) (1996) 189–194.
[40] D. Gedeon, Mean-parameter modeling of oscillating flow, J. Heat Transfer 108 (1986) 513–518.
[41] S.V. Patankar, Numerical Heat Transfer and Fluid Flow, Hemisphere Publishing Corporation, New York, 1980.
[42] J.P. Van Doormaal, G.D. Raithby, Enhancements of the SIMPLE method for predicting incompressible fluid flows, Numer. Heat Transfer 7 (1984) 147–163.
[43] F.M. White, Viscous Fluid Flow, second ed., McGraw-Hill, Inc., NY, 1991.
[44] W.M. Kays, M.E. Crawford, Convective Heat and Mass Transfer, third ed., McGraw-Hill, NY, 1993.
[45] B.S. Petukhov, Heat transfer and friction in turbulent pipe flow with variable physical properties, Advances in Heat Transfer, vol. 6, Academic Press, New York, 1970, pp. 504–564.
[46] B.S. Petukhov, V.N.N. Popov, Theoretical calculation of heat exchange and frictional resistance in turbulent flow in tubes of incompressible fluid with variable physical properties, High Temp. 1 (1963) 69–83.
[47] J.E. Dec, J.O. Keller, I. Hongo, Time-resolved velocities and turbulence in the oscillating flow of a pulse combustor tail pipe, Combust. Flame 83 (1991) 271–292.
[48] J.E. Dec, J.O. Keller, Time-resolved gas temperatures in the oscillating turbulent flow of a pulse combustor tail pipe, Combust. Flame 80 (1990) 358–370.
[49] S. Uchida, The pulsating viscous flow superposed on the steady laminar motion of incompressible fluid in a circular pipe, ZAMP 7 (1956) 403–422.